

Polymer Chemistry

Accepted Manuscript



This is an *Accepted Manuscript*, which has been through the Royal Society of Chemistry peer review process and has been accepted for publication.

Accepted Manuscripts are published online shortly after acceptance, before technical editing, formatting and proof reading. Using this free service, authors can make their results available to the community, in citable form, before we publish the edited article. We will replace this *Accepted Manuscript* with the edited and formatted *Advance Article* as soon as it is available.

You can find more information about *Accepted Manuscripts* in the [Information for Authors](#).

Please note that technical editing may introduce minor changes to the text and/or graphics, which may alter content. The journal's standard [Terms & Conditions](#) and the [Ethical guidelines](#) still apply. In no event shall the Royal Society of Chemistry be held responsible for any errors or omissions in this *Accepted Manuscript* or any consequences arising from the use of any information it contains.

ARTICLE

Macroporous antibacterial hydrogels with tunable pore structures fabricated by using Pickering high internal phase emulsions as templates

Cite this: DOI: 10.1039/x0xx00000x

Received 00th January 2012,
Accepted 00th January 2012

DOI: 10.1039/x0xx00000x

www.rsc.org/

Shengwen Zou^a, Zengjiang Wei^a, Yang Hu^a, Yonghong Deng^{b,*}, Zhen Tong^a, and Chaoyang Wang^{a,*}

Artemisia argyi oil (AAO)-loaded macroporous antibacterial hydrogels were prepared by polymerization of oil-in-water Pickering high internal phase emulsions (HIPEs). The HIPEs were stabilized by the synergy of hydrophilic silica nanoparticles (N20) and surfactant Tween 80. The void interconnectivity and pore size of the hydrogels could be tailored readily by varying the concentrations of N20 nanoparticle and Tween 80. The mechanical property of the porous hydrogels was related to the pore structure of the materials. There was an optimal condition of the N20 particle and Tween 80 contents where the hydrogel exhibited high compressive stress and strain. The in vitro release of the AAO-loaded hydrogels with different inner morphologies was evaluated and showed controlled release activity. The antibacterial activity of the AAO-loaded hydrogel was evaluated against *Staphylococcus aureus* and *Escherichia coli*. This kind of hydrogel exhibited excellent and long-term antibacterial activity indicating their potential usage in biomedical and infection prevention applications.

Introduction

Porous hydrogels with well-defined pore structure have attracted considerable attention due to their multifarious applications such as scaffolds for tissue engineering,^{1,2} vehicles for drug delivery^{3,4} and self-healing materials.^{5,6} CO₂-in-water (C/W) high internal phase emulsions (HIPEs)^{7,8} and oil-in-water (O/W) HIPEs^{9,10} are considered as very effective templates to produce such kind of high porosity hydrogels. HIPEs as unique emulsions with the internal phase fractions (IPFs) more than 74 vol% of the total emulsion volume are well known to all of us, and PolyHIPEs are usually synthesized by polymerizing the monomers in the continuous phase of HIPEs and then removing the dispersed phase.¹¹⁻¹⁵ However, the preparation of C/W HIPEs requires specialized equipment to achieve the required pressures.^{7,8} And therefore O/W HIPEs instead of C/W HIPEs were most widely investigated as templates for the fabrication of macroporous hydrogels.^{3,16} Unfortunately, compared with water-in-oil (W/O) HIPEs, there are some difficulties for the preparation of O/W HIPEs and the subsequent hydrophilic polyHIPEs, like poor stability of O/W HIPEs and hard disposing of organic internal phase.¹⁷ On the other hand, there is also a big waste of the internal oil phase due to the direct washing in the post treatment.

In most cases, the O/W HIPEs are stabilized by large amount of surfactants at high concentrations of 5-50 vol%, where the enormous quantity of surfactants presents economic and potential environmental problems.¹⁸⁻²¹ Therefore, much more attentions are focus on the Pickering-HIPEs, which are stabilized by colloidal particles instead of traditional surfactants.²²⁻²⁶ Not only less emulsifier dose required for emulsions, but also Pickering emulsion droplets exhibit better stabilization against coalescence.²⁷⁻³⁴ Finally polyHIPEs with particle decorated pore walls are obtain. This layer of particles can introduce additional functionalities which may lead to numerous applications in the future.³⁵⁻³⁷ Although there are some reports on the O/W Pickering HIPEs,^{24,38,39} few work focuses on the synthesis of the corresponding poly-Pickering-HIPEs.⁴⁰⁻⁴² Moreover, it is usually a challenge to obtain the particles just with the right hydrophilicity that can be used as stabilizers for HIPEs. However, in our previous work, we found that the co-emulsifier system of nanoparticles and surfactants exhibited synergism in preparation of stable W/O HIPEs, and could tailor the pore morphology of the polyHIPEs by varying the relative concentration of particles and surfactants.⁴³ Therefore, the use of co-stabilizers of nanoparticles and surfactants would also be a good strategy to prepare O/W HIPEs.

Artemisia argyi oil (AAO), the main medicinal component of artemisia argyi, is an important raw material used in cosmetics, pharmaceuticals and perfume products, due to its wide range uses of antibacterial, antifungal, anti-inflammatory.⁴⁴ The main compositions of AAO are ethers, alcohols, ketones, monoterpenes and sesquiterpenes.^{44,45} AAO is volatile in the presence of air, light and heat, which greatly limits its application. Hence, AAO as the internal oil phase encapsulated in polyHIPEs seem to be a good choice to prolong the efficiency and expand the potentials of AAO applications. Meanwhile, this functional oil in the polyHIPEs doesn't need to be washed out, which overcomes the drawback of the significant waste of the oil phase.

Herein, we employed hydrophilic silica nanoparticle (N20) and surfactant of Tween 80 as co-stabilizers to prepare O/W HIPEs with functional AAO as the oil phase. The macroporous antimicrobial hydrogels were one pot fabricated after the polymerization of monomer in the continuous phase. The effects of N20 particle and Tween 80 concentrations on the emulsion morphology, pore structure of polyHIPEs, mechanical property of the hydrogels are discussed in detail. Furthermore, the release behavior and antimicrobial activity of the AAO-loaded hydrogels were also evaluated. This co-emulsifier system of particle and surfactant should be an excellent route to fabricate pore structure and size controllable polyHIPEs. Besides, the as-prepared AAO-loaded hydrogels provided promising applications in biomedical fields.

Experimental

Materials

Acrylamide (AM) was purchased from Tianjin Yongda Chemical Reagent, China. *N,N'*-methylene bisacrylamide (BIS) was obtained from Acros Organics and used as received. Initiator potassium persulphate ($K_2S_2O_8$) was recrystallized twice before use. Tween 80 was bought from Tianjin Kermel Chemical Reagent, China. AAO was purchased from Jiangxi Jishui Kangshen Natural Medicinal Oil Refinery, China. Silica N20 with an average diameter of 20 nm was a gift from Wacker, Germany. Pure water was produced by deionization and filtration using a Millipore purification apparatus (resistivity >18.2 M Ω -cm).

Preparation of macroporous PAM hydrogels

In a typical process, N20 nanoparticles were initially dispersed into 1 mL aqueous solution of surfactant Tween 80. Then, the monomer AM (200 mg), the cross-linker BIS (20 mg) and the initiator KPS (10 mg) were dissolved in the above N20 nanoparticles dispersion. The HIPE was prepared by adding AAO to the water phase in batches and then hand shaking at every turn. It was worth noting that high speed homogenizing the oil and water phase or hand shaking the total oil with water cannot obtain HIPE. The as-prepared HIPE was then transferred to a glass tube with 15 mm diameter \times 100 mm length, and polymerized in a 60 °C oven for 12 h. The polymerized material was removed from the mould and could be used for compression test, release and antimicrobial activities. The detail parameters and characterization of all samples are listed in **Table 1**.

For SEM observation, the polyHIPEs were washed with ethanol to remove any impurities, followed by drying to constant weight at room temperature.

Compression test

Compression test was carried out on the as-prepared AAO-loaded hydrogel samples with a Shimadzu AG-X plus testing system at 25 °C. For the compression test, the sample was 15 mm diameter \times 10 mm thickness. All the samples were mounted very carefully in the compression fixture without any damage. The samples were compressed to break at a constant speed of 1 mm/min. The compressive strain was taken as the thickness change relative to the initial thickness of the specimen, and the compressive stress was evaluated on the area of the initial cross section. The Young's modulus *E* was estimated from the stress vs. strain curve. For every test, 2-5 samples were used for average.

In vitro release

In the in vitro release experiments, the AAO-loaded PAM hydrogels were cut into disks with 15 mm diameter \times 2 mm thickness, each weighing W_a g. And then, the hydrogels were placed in an oven with a specific temperature to release the AAO. At predetermined time intervals, the samples were taken out and weighed to obtain the residual weight of the hydrogel disks (W_b g). All determinations were carried out in triplicate, and the mean values were calculated. The cumulative release rate (*CR*) was determined by the following formula:

Table 1 Composition of templates and characterization of the resulted hydrogels.

Sample ^a	N20 (wt%) ^b	Tween80 (wt%) ^b	Emulsion size (μ m)	Strain (%)	Stress (kPa)	Pore type
1	2	0	94 \pm 10	40 \pm 4	30 \pm 10	Closed
2	2	2	49 \pm 7	77 \pm 5	234 \pm 10	Closed-open
3	2	5	25 \pm 5	64 \pm 3	95 \pm 6	Open
4	0	5	18 \pm 4	51 \pm 4	53 \pm 8	Open
5	1	5	20 \pm 4	63 \pm 5	62 \pm 7	Open
6	4	5	28 \pm 6	85 \pm 3	339 \pm 8	Closed-open
7 ^c	2	2	—	31 \pm 4	103 \pm 10	Closed

^aThe internal phase fraction of all HIPEs was 80 vol%. ^bWith respect to the continuous phase. ^cControl experiment with no oil.

$$CR = \frac{W_a - W_b}{W_a} \times 100\% \quad (1)$$

Antibacterial activity of AAO-loaded porous PAM hydrogels

The antibacterial activities of AAO-loaded PAM hydrogels were tested by an inhibition zone method. In this method, *Staphylococcus aureus* (*S. aureus*) and *Escherichia coli* (*E. coli*) were taken as the model bacteria. For this study, the samples (AAO-loaded PAM hydrogels, PAM hydrogel without AAO of sample 7 as control) were cut into small pieces (15 mm diameter \times 2 mm thickness) and the antimicrobial activity was tested using modified agar diffusion assay (disc test). The plates were examined for possible clear zone formation after incubation at 37 °C for predetermined time intervals. The presence of clear zone around hydrogel discs on the plates was recorded as an inhibition against the microbial species.

Characterization

Photographs of emulsion vials and porous hydrogel samples were captured by a digital camera (IXUS 220HS, Canon). The high internal phase emulsions were observed with a microscope (Carl Zeiss, German). The average diameter of the emulsion droplets was determined with a laser scattering particle size distribution analyzer (Malvern mastersizer 2000). The morphology of Au-coated porous materials was obtained using a Zeiss EVO 18 scanning electron microscope (SEM) operating at 10 kV.

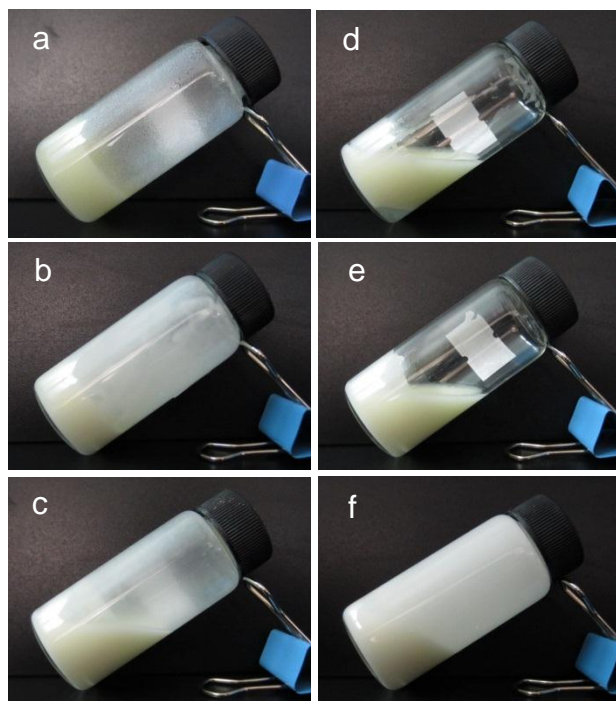


Fig. 1 Digital photos of AAO-in-water HIPEs stabilized by co-stabilizer of N20 nanoparticles and Tween 80: (a-c) N20 concentration was fixed at 2 wt% and Tween 80 was 0 wt%, 2 wt% and 5 wt%, respectively; (d-f) Tween 80 content was fixed at 5 wt% and N20 was 0 wt%, 1wt% and 4 wt%, respectively. All internal phase fractions are 80 vol%.

Results and discussion

Preparation of HIPEs

In our previous work,⁴³ we had provided an efficient route to obtain water-in-oil (W/O) HIPEs with internal phase fraction exceeding 98 vol% by using hydrophobic silica nanoparticles (H30) and surfactant of sorbitan trioleate (Span 85) as co-stabilizers. The synergistic effect between the particles and surfactant existed and played a great role in stabilizing HIPEs. More importantly, the polyHIPEs with different pore structure can be acquired by adjusting the ratios of nanoparticle to surfactant. In this study, we attempted to prepare oil-in-water (O/W) HIPEs employed AAO as functional oil phase stabilized by hydrophilic silica nanoparticles (N20) and surfactant of Tween 80. The HIPEs with different concentrations of N20 and Tween 80 were described in Table 1. The digital photographs of these HIPEs are shown in **Fig. 1**. It can be found that typical gel like AAO-in-water HIPEs were formed even solely stabilized by 2 wt% of N20 particles. The high viscosity resulted in no flow emulsions even the vial was inclined. By introducing surfactant Tween 80 as costabilizer, HIPEs with lower viscosities were obtained as the emulsions flowed along the tilt directions (Fig. 1a-c). The HIPEs solely stabilized by Tween 80 can also be prepared but exhibited weak unstability with slight phase separation. However, the stability was enhanced with the addition of N20 nanoparticles due to the particle layer surrounding the droplets ensure the emulsions mechanically stabilized against coalescence.²⁴

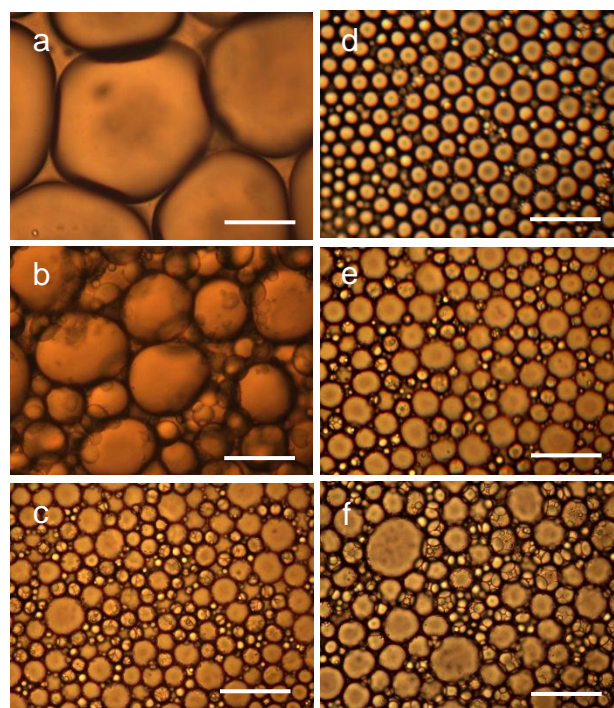


Fig. 2 Optical images of AAO-in-water HIPEs stabilized by co-stabilizers of N20 nanoparticles and Tween 80: (a-c) N20 concentration was fixed at 2 wt% and Tween 80 was 0 wt%, 2 wt% and 5 wt%, respectively; (d-f) Tween 80 content was fixed at 5 wt% and N20 was 0 wt%, 1wt% and 4 wt%, respectively. All internal phase fractions are 80 vol% and scale bars are 50 μ m.

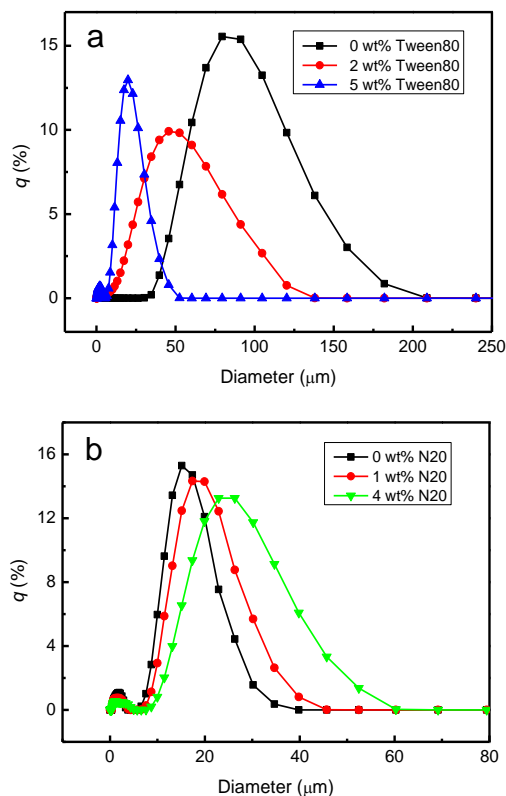


Fig. 3 Size distribution of AAO-in-water HIPEs stabilized by co-stabilizers of N20 nanoparticles and Tween 80: (a) different Tween 80 concentrations when fixed the N20 concentration at 2 wt%; (b) different N20 contents while Tween 80 content was fixed at 5 wt%.

Then, a series of HIPE droplets were observed by optical microscope, also their average diameter and the size distribution were calculated by a laser scattering particle size distribution analyzer. The optical images of HIPEs are shown in **Fig. 2**. From a to c, the Tween 80 content in continuous phase increased from 0 to 5 wt% and with a constant N20 concentration of 2 wt%. With the increasing of surfactant Tween 80, the size of these droplets decreased from 95 to 26 μm (**Fig. 3**), and the droplet shape changed from deformed sphere to well-defined spherical. It was noting for that the viscosity of the emulsions decreased detectably with the addition of Tween 80 that had been discussed above. There was some literature reported that stable Pickering emulsions can only be formed if the particles were weakly flocculated to some extent.⁴⁶⁻⁴⁸ However, the addition of surfactant to particle dispersion would prevent the excess particles from aggregating. As a result, the system viscosity declined and resulted in smaller size, spherical shape emulsions. Besides, the surfactant may also adsorb on the particles that leads to the promotion of particle's ability to stabilize emulsion. In this case, original particle-stabilized big droplets broke up to form many small ones. The effect of particle content on the emulsion was studied with various contents from 0 to 4 wt% when fixed Tween 80 at 5 wt%. The emulsion exhibited good spherical morphology

until the high particle concentration of 2 wt%. The average size gradually increased from 19 to 28 μm and the emulsion stability was enhanced significantly with the rising particle content. The reason for it is that the droplet size of the emulsion solely stabilized by N20 (95 μm) is much bigger than that by Tween 80 (19 μm). On the other hand, the size distributions of all Pickering HIPE droplets revealed to be polydisperse. This polydispersity is consistent with the previous reported Pickering HIPEs.²²⁻²⁴

Fabrication of porous polyHIPEs

The PAM foams were obtained by translating the HIPEs containing AM, BIS and KPS into an oven and polymerizing at 60 $^{\circ}\text{C}$ for 12 h. The products were purified by ethanol to remove the AAO and air-dried at room temperature for SEM test. **Fig. 4** presents the SEM images of PAM foams prepared under different concentrations of N20 and Tween 80 (Table 1). It was found that the closed-pore structure appeared when the HIPEs template was solely stabilized by 2 wt% of N20 particles. The void diameter of this poly-Pickering-HIPE was about 100 μm which was much larger than that of the conventional poly-surfactant-HIPE (Fig. 4a, d). The large void porous materials were good candidates for scaffold and tissue engineering.^{49,50} However, the closed-cell structure of these poly-Pickering-HIPE, which made it difficult to remove the internal oil phase and limited their biological applications.^{51,52} The closed pore structure of poly-Pickering-HIPE may be due to the particles surrounding the droplets thickly that hindered the formation of interconnecting pores during polymerization and/or post treatment. As expect, a series of open-cell foams were obtained by adding Tween 80 with concentration ranging from 2 to 5 wt% when N20 nanoparticle was kept at 2 wt%. It was found that the void size of the sample with 2 wt% Tween 80 was decreased significantly and the larger voids were surrounded by some smaller ones. Moreover, compared with the morphology of sample 1 solely stabilized by 2 wt% N20 particles, sample 2 possessed obvious interconnecting pores (denoted as pore throats) on the void walls. When the Tween 80 content increased to 5 wt%, the void size became homogeneous and much smaller. And it was worth to be noted that the pore throats were spread on the void walls and the interconnecting degree was close to that of conventional polyHIPE of sample 4.

As seen in Fig. 4, at constant Tween 80 concentration of 5 wt% in the continuous phase, adjusting N20 particle concentration from 1 to 4 wt% caused a steady increase in average void size. The observation was consistent with that found in the corresponding emulsion templates, indicating that the good emulsion stability during the curing process. Furthermore, increasing the amount of N20 particle rendered the number of pore throats on the void walls gradually decreased. This should be owing to excessive nanoparticles could render the particle layers at the oil-water interfaces thicker and thereby making the formation of interconnecting pores harder. In short, various pore sizes and interconnecting degree of PAM foams can be readily fabricated by adjusting the ratio of N20 particle to Tween 80.

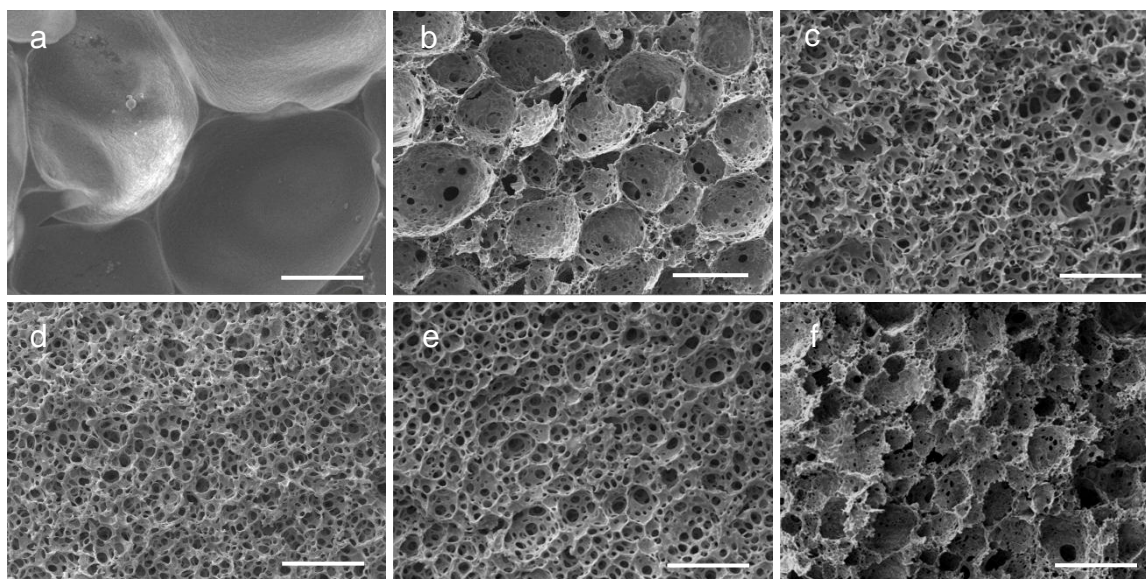


Fig. 4 SEM images of PAM foams fabricated from HIPEs which were stabilized by co-stabilizers of N20 nanoparticles and Tween 80: (a-c) N20 concentration was fixed at 2 wt% and Tween 80 was 0 wt%, 2 wt% and 5 wt%, respectively; (d-f) Tween 80 content was fixed at 5 wt% and N20 was 0 wt%, 1wt% and 4 wt%, respectively. All internal phase fractions are 80 vol% and scale bars are 40 μm .

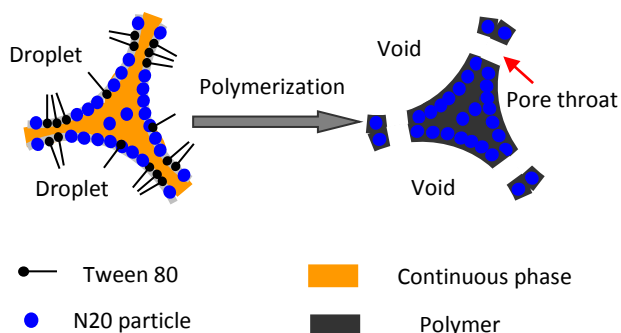


Fig. 5 Schematic illustration of the formation of open cell structure hydrogels with nanoparticle and surfactant as co-emulsifiers.

The possible formation of open cell structure of hydrogels containing both N20 particles and Tween 80 is schematically presented in **Fig. 5**. There are nanoparticles and surfactant molecules coexisting in the continuous phase, which makes competitive adsorption on to the oil-water interface.^{50,53} The partial adsorption of surfactant on the surface of droplets substantially reduced the interfacial tension. As a result, the droplet size decreased and increased the number of contact points among adjacent droplets. It should be noted that the continuous phase film at the contact point was thinner than that of the trigonal region. Therefore, the surfactant molecules preferred to migrate to contact points due to their small sizes, leaving larger size particles adsorb on oil-water interface of trigonal regions. The more surfactant the thinner the continuous phase films, leading to more easily form pore throats during the solidification of the continuous phase.

Mechanical properties

The AAO loaded macroporous hydrogels exhibited good compressive resistance as shown in **Fig. 6**. The hydrogel can recover its original shape quickly after removal of the compression force. Then, AAO-loaded macroporous PAM hydrogels containing various concentrations of N20 particle and Tween 80 were taken for compressive test. Representative compressive stress-strain curves for the AAO-loaded PAM hydrogels are shown in **Fig. 7**. For sample 1 solely stabilized by 2 wt% N20, the stress-strain curve showed small strain and stress, indicating the brittleness of the sample with high particle content. This may be due to the closed structure of big polymer cell that encapsulating AAO, resulting in difficult deformation unless the closed cell broken. When adding 2 wt% Tween 80 as co-stabilizer, the resultant AAO-loaded hydrogel exhibited a significant increase in both strain and stress. Tracing to the structures of the two samples, sample 2 had some small pore throats on void walls while sample 1 had only big closed cell. The small pore throats can make the oil phase gradually output under compression that resulted in the compressive strain up to 77%. On the other hand, the embed nanoparticles in polymer wall enhanced the materials with high stress (234 kPa). However, there was an optimal ratio of particle to surfactant, higher Tween 80 concentration of 5 wt% made the reduction of stress and strain. It worth noted that sample 4 stabilized solely by 5 wt% Tween 80 also had small stress and strain. Interestingly, the modulus can also be significantly increased by adding appropriate amount of N20 particle.

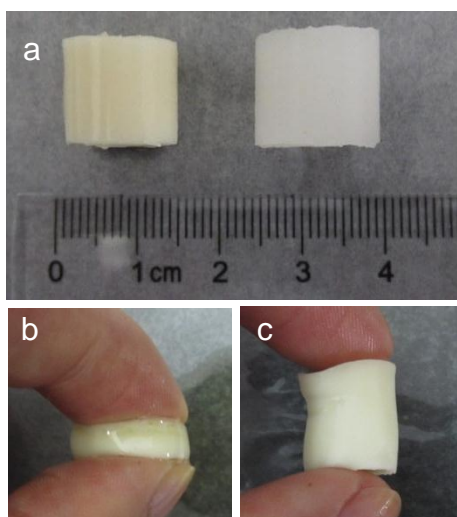


Fig. 6 (a) AAO-loaded porous PAM hydrogel (left) and no AAO loaded PAM hydrogel (right); (b) AAO-loaded porous hydrogel was compressed and (c) recovered after the removal of compression force.

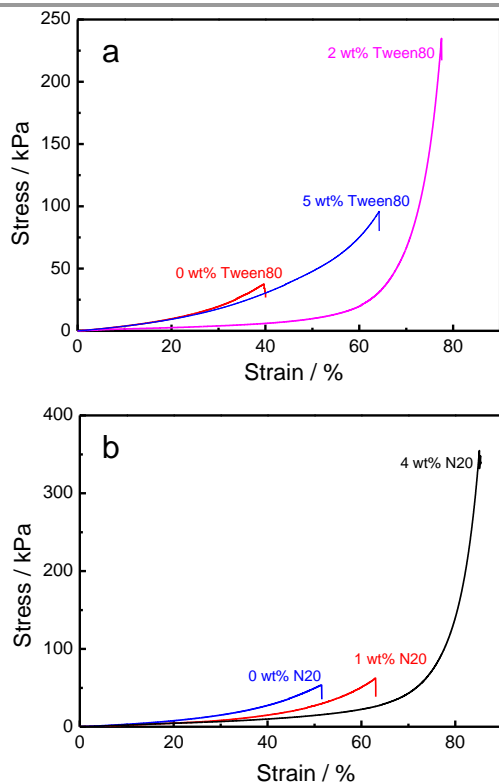


Fig. 7 Compressive stress-strain curves for AAO-loaded hydrogels synthesized from HIPEs which were stabilized by co-stabilizers of N20 nanoparticles and Tween 80: (a) different Tween 80 concentrations when fixed the N20 concentration at 2 wt%; (b) different N20 contents while Tween 80 content was fixed at 5 wt%.

By contrast, we synthesized a conventional PAM hydrogel without emulsion template (details can be seen in Table 1, sample 7). The stress-strain curve is presented in **Fig. 8**. The sample was brittle and showed very low stress and compression

ratio compared to that of sample 2. This indicated that AAO within the hydrogels had benefit to improve the mechanical property of the polyHIPEs. The internal structure of the conventional hydrogel was revealed by SEM imaging. This hydrogel had similar closed pore structure to the sample 1 but with smaller pore size about 10 μm . The closed pore structure may also be the main reason of the poor mechanical property.

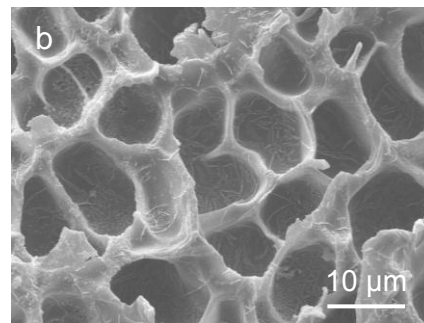
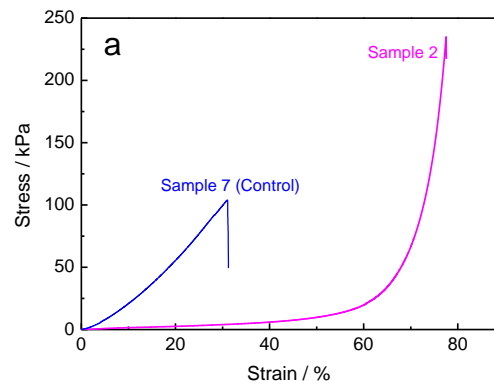


Fig. 8 (a) Compressive stress-strain curves for AAO-loaded hydrogel (sample 2) and no AAO loaded hydrogel (sample 7); (b) SEM image of no AAO loaded hydrogel.

In vitro release study

The release behaviour of AAO and water from the hydrogels with different pore structures was investigated at 37 $^{\circ}\text{C}$ in an oven. The release profiles are shown in **Fig. 9**. The release included the volatilization of both AAO and water. The volatilization of water is weaker than AAO. The water content of all hydrogels was almost the same, about 20%, with respect to the mass of oil-loaded PAM hydrogels. The total release could reflect the volatilization rate of AAO. It can be seen that the release rates of AAO from sample 2 and sample 4 were relatively fast in the first stage (within the first 24 h), and next experienced an appreciably slow release rate period. The initial weak “burst effect” was primarily attributed to a fast release of AAO on the surface and near the interior surface.⁵⁴ In the later stage, the slower release was ascribed to the decrease in the concentration of AAO within the near surface of the macroporous hydrogel. As expect, sample 1 had a relatively slow release rate in the early stage due to the completely closed-cell structure compared to the other samples. However,

the release rate did not seem to decrease in the later stage. The possible reason was the obvious cracks caused in the release process, which enhanced AAO release from the sample. Furthermore, the release rate of AAO decreased significantly with lowering the temperature (Fig. 9d). This was attributed to the fact that the volatility of AAO weakened with decreasing the temperature.

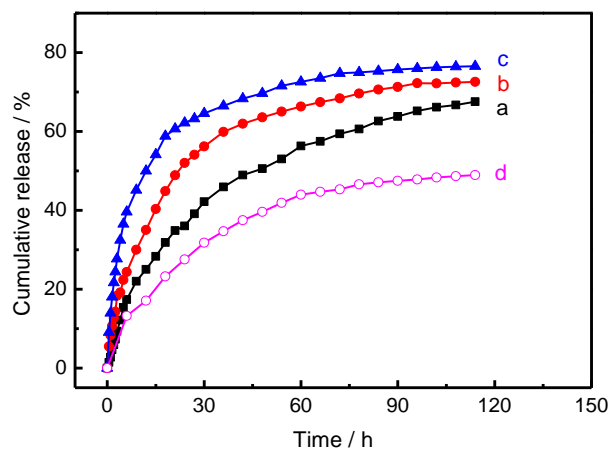


Fig. 9 Release profiles of AAO-loaded hydrogels with different pore structure at 37 °C: (a) sample 1 with closed cell structure, (b) sample 2 with closed-open cell, and (c) sample 4 with open cell structure. (d) The release profile of sample 2 at 25 °C.

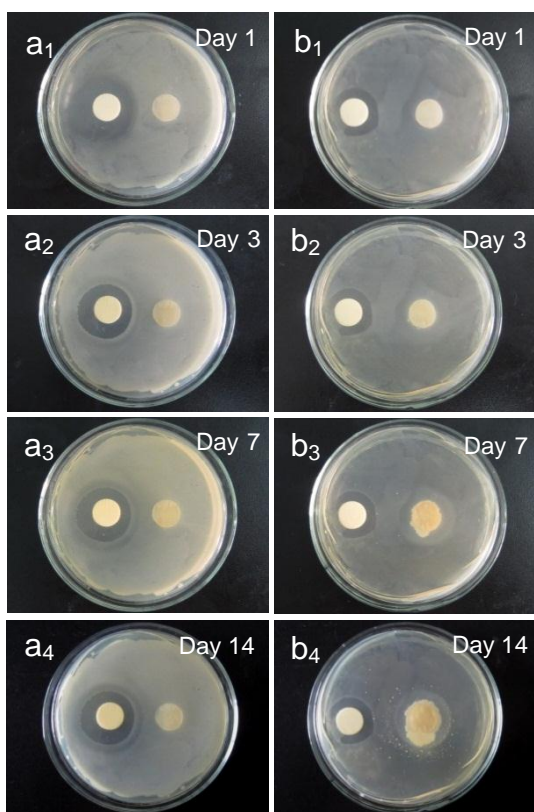


Fig. 10 Antibacterial activity of AAO-loaded hydrogels (sample 2) with different storage time against *S. aureus* (left column) and *E. coli* (right column).

Antibacterial activity study

The antimicrobial activities of AAO-loaded hydrogels with different storage times against *S. aureus* and *E. coli* were investigated (Fig. 10). The sample 2 with appropriate pore structure and good mechanical property was selected for the antimicrobial test, the hydrogel without AAO (sample 7) as a control. The results showed that the AAO-loaded hydrogel exhibited significant reduction of *S. aureus* and *E. coli* growth. This was ascribed to the fast release of AAO into the media. According to the Standard Antibacterial test “SNV 195920-1992”, more than 1 mm microbial zone inhibition can be considered as a good antibacterial product.⁵⁵ The AAO-loaded hydrogel developed in the present investigation have exhibited > 4 mm inhibition zone in all the cases even after storage for 2 weeks. It demonstrated that the AAO-loaded hydrogels had excellent and long-term antimicrobial effect. In addition, it was observed that the antibacterial effect against *E. coli* was slightly lower than that against *S. aureus*. The reason was that compared with *S. aureus*, *E. coli* had an outer membrane outside the peptidoglycan layer, which could protect the bacteria cell from attacking by extraneous compounds in certain degree.^{56,57}

Conclusions

Macroporous antimicrobial PAM hydrogels were one pot fabricated by in situ polymerization of AAO-in-water HIPES templates stabilized by silica N20 nanoparticles and surfactant Tween 80. It was found that adding Tween 80 to the Pickering HIPES, the pore structure of the polyHIPES varied from closed-cell to open-cell. Moreover, the interconnectivity and average pore size could be tailored by varying the relative concentrations of N20 particles and Tween 80. The mechanical properties of the polyHIPES could be controlled by altering the material morphology which was also dependent on the ratio of nanoparticle to surfactant. The hydrogel exhibited a high compressive stress of 234.6 kPa and 77.5% strain when using 2 wt% N20 and 2 wt% Tween 80 as co-stabilizer. In vitro release of the AAO-loaded hydrogels showed different release profiles depending on various pore structure and temperature, indicating good controlled release activity of these materials. Furthermore, the AAO-loaded macroporous hydrogels exhibited excellent and long term antimicrobial activity against both *S. aureus* and *E. coli*. Overall, it has been shown that the AAO-loaded macroporous hydrogels are potentially suitable materials for biomedical fields. Further work will explore the fabrication of the AAO-loaded hydrogels into different shapes, with a view to find more practical applications.

Acknowledgements

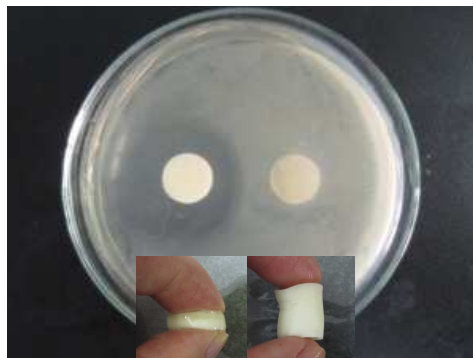
This work was financially supported by the National Natural Basic Research Program of China (973 Program, 2012CB821500), the National Natural Science Foundation of China (21274046) and the Natural Science Foundation of Guangdong Province (S2012020011057).

Notes and references

- ^aResearch Institute of Materials Science, South China University of Technology, Guangzhou 510640, China. E-mail: zhywang@scut.edu.cn; Tel & Fax: +86-20-22236269;
- ^bSchool of Chemistry and Chemical Engineering, South China University of Technology, Guangzhou 510640, China. E-mail: yhdeng@scut.edu.cn; Tel: +86-20-87114722; Fax: +86-20-87114721.
- 1 Q. Hou, P. A. D. Bank and K. M. Shakesheff, *J. Mater. Chem.*, 2004, **14**, 1915–1923.
 - 2 J. H. Scott, *Adv. Mater.*, 2009, **21**, 3330–3342.
 - 3 T. Trongsatitkul and B. M. Budhlall, *Polym. Chem.*, 2013, **4**, 1502–1516.
 - 4 T. R. Hoare and D. S. Kohane, *Polymer*, 2008, **49**, 1993–2007.
 - 5 B. Yang, Y. L. Zhang, X. Y. Zhang, L. Tao, S. X. Li and Y. Wei, *Polym. Chem.*, 2012, **3**, 3235–3238.
 - 6 Z. J. Wei, J. He, T. Liang, H. Oh, J. Athas, Z. Tong, C. Y. Wang and Z. H. Nie, *Polym. Chem.*, 2013, **4**, 4601–4605.
 - 7 R. Butler, C. M. Davies and A. I. Cooper, *Adv. Mater.*, 2001, **13**, 1459–1463.
 - 8 R. Butler, I. Hopkinson and A. I. Cooper, *J. Am. Chem. Soc.*, 2003, **125**, 14473–14481.
 - 9 S. Arditty, C. P. Whitby, B. P. Binks, V. Schmitt and F. Leal-Calderon, *Eur. Phys. J. E*, 2003, **11**, 273–281.
 - 10 S. Kovačič, D. Štefanec and P. Krajnc, *Macromolecules*, 2007, **40**, 8056–8060.
 - 11 N. R. Cameron and D. C. Sherrington, *Adv. Polym. Sci.*, 1996, **126**, 163–214.
 - 12 I. Pulko and P. Krajnc, *Chem. Commun.*, 2008, 4481–4483.
 - 13 S. Kovačič, P. Krajnc and C. Slugovc, *Chem. Commun.*, 2010, **46**, 7504–7506.
 - 14 T. S. Dunstan and P. D. I. Fletcher, *Langmuir*, 2011, **27**, 3409–3415.
 - 15 T. S. Dunstan, P. D. I. Fletcher and S. Mashinchi, *Langmuir*, 2012, **28**, 339–349.
 - 16 A. Barbetta, M. Massimi, B. Di Rosario, S. Nardecchia, M. De Colli, L. C. Devirgiliis and M. Dentini, *Biomacromolecules*, 2008, **9**, 2844–2856.
 - 17 S. Livshin and M. S. Silverstein, *J. Polym. Sci. Part A: Polym. Chem.*, 2009, **47**, 4840–4845.
 - 18 P. Krajnc, D. Štefanec and I. Pulko, *Macromol. Rapid Commun.*, 2005, **16**, 1289–1293.
 - 19 F. Fernández-Trillo, J. C. M. van Hest, J. C. Thies, T. Michon and N. R. Cameron, *Adv. Mater.*, 2009, **21**, 55–59.
 - 20 S. D. Kimmins and N. R. Cameron, *Adv. Funct. Mater.*, 2011, **21**, 211–225.
 - 21 D. W. Johnson, C. Sherborne, M. P. Didsbury, C. Pateman, N. R. Cameron and F. Claeysens, *Adv. Mater.*, 2013, **25**, 3178–3181.
 - 22 A. Menner, V. Ikem, M. Salgueiro, M. S. P. Shaffer and A. Bismarck, *Chem. Commun.*, 2007, 4274–4276.
 - 23 V. O. Ikem, A. Menner and A. Bismarck, *Angew. Chem., Int. Ed.*, 2008, **47**, 8277–8279.
 - 24 Z. F. Li, T. Ming, J. F. Wang and T. Ngai, *Angew. Chem. Int. Ed.*, 2009, **48**, 8490–8493.
 - 25 G. Q. Sun, Z. F. Li and T. Ngai, *Angew. Chem., Int. Ed.*, 2010, **49**, 2163–2166.
 - 26 Y. H. Chen, N. Ballard, F. Gayet and S. A. F. Bon, *Chem. Commun.*, 2012, **48**, 1117–1119.
 - 27 S. Fujii, E. S. Read, B. P. Binks and S. P. Armes, *Adv. Mater.*, 2005, **17**, 1014–1018.
 - 28 K. L. Thompson, P. Chambon, R. Verber and S. P. Armes, *J. Am. Chem. Soc.*, 2012, **134**, 12450–12453.
 - 29 Q. X. Gao, C. Y. Wang, H. X. Liu, Y. H. Chen and Zhen Tong, *Polym. Chem.*, 2010, **1**, 75–77.
 - 30 Z. Zheng, X. H. Zheng, H. T. Wang and Q. G. Du, *ACS Appl. Mater. Interfaces*, 2013, **5**, 7974–7982.
 - 31 N. Ballard and S. A. F. Bon, *Polym. Chem.*, 2011, **2**, 823–827.
 - 32 J. Tian, G. N. Liu, C. Guan and H. Y. Zhao, *Polym. Chem.*, 2013, **4**, 1913–1920.
 - 33 G. N. Yin, Z. Zheng, H. T. Wang, Q. G. Du and H. D. Zhang, *J. Colloid Interface Sci.*, 2013, **394**, 192–198.
 - 34 Y. Yang, Y. Ning, C. Y. Wang and Z. Tong, *Polym. Chem.*, 2013, **4**, 5407–5415.
 - 35 M. C. Hermant, B. Klumperman and C. E. Koning, *Chem. Commun.*, 2009, 2738–2740.
 - 36 T. T. Li, H. R. Liu, L. Zeng, S. Yang, Z. C. Li, J. D. Zhang and X. T. Zhou, *J. Mater. Chem.*, 2011, **21**, 12865–12872.
 - 37 A. V Ichez, C. Rodríguez-Abreu, J. Esquena, A. Menner and A. Bismarck, *Langmuir*, 2011, **27**, 13342–13352.
 - 38 Q. J. Chen, Y. Y. Xu, X. T. Cao, L. J. Qin and Z. S. An, *Polym. Chem.*, 2014, **5**, 175–185.
 - 39 H. Liu and C. Y. Wang, *RSC Adv.*, 2014, **4**, 3864–3872.
 - 40 Q. J. Chen, X. T. Cao, H. Liu, W. Zhou, L. J. Qin and Z. S. An, *Polym. Chem.*, 2013, **4**, 4092–4102.
 - 41 S. Z. Zhou, A. Bismarck and J. H. G. Steinke, *J. Mater. Chem.*, 2012, **22**, 18824–18829.
 - 42 Y. Yang, Z. J. Wei, C. Y. Wang and Z. Tong, *Chem. Commun.*, 2013, **49**, 7144–7146.
 - 43 S. W. Zou, Y. Yang, H. Liu and C. Y. Wang, *Colloids Surf. A*, 2013, **436**, 1–9.
 - 44 H. C. Huang, H. F. Wang, K. H. Yih, L. Z. Chang and T. M. Chang, *Int. J. Mol. Sci.*, 2012, **13**, 14679–14697.
 - 45 N. Li, Y. Mao, C. H. Deng and X. M. Zhang, *J. Chromatogr. Sci.*, 2008, **46**, 401–405.
 - 46 E. H. Lucassen-Reynders and M. van den Tempel, *J. Phys. Chem.*, 1963, **67**, 731–734.
 - 47 B. P. Binks, *Curr. Opin. Colloid Interface Sci.*, 2002, **7**, 21–41.
 - 48 S. W. Zou, H. Liu, Y. Yang, Z. J. Wei and C. Y. Wang, *React. Funct. Polym.*, 2013, **73**, 1231–1241.
 - 49 S. Caldwell, D. W. Johnson, M. P. Didsbury, B. A. Murray, J. J. Wu, S. A. Przyborski and N. R. Cameron, *Soft Matter*, 2012, **8**, 10344–10351.
 - 50 Y. Hua, S. M. Zhang, Y. Zhu, Y. Q. Chu and J. D. Chen, *J. Polym. Sci. Part A: Polym. Chem.*, 2013, **51**, 2181–2187.
 - 51 G. M. Akay, A. Birch, M. A. Bokhari, *Biomaterials*, 2004, **25**, 3991–4000.
 - 52 M. Bokhari, R. J. Carnachan, S. A. Przyborski, Cameron N. R. J. *Mater. Chem.*, 2007, **17**, 4088–4094.
 - 53 V. O. Ikem, A. Menner, T. S. Horozov, and A. Bismarck, *Adv. Mater.* 2010, **22**, 3588–3592.
 - 54 Y. Hu, Y. Yang, Y. Ning, C. Y. Wang and Z. Tong, *Colloids Surf., B*, 2013, **112**, 96–102.

- 55 S. Ravindra, Y. M. Mohan, N. N. Reddy and K. M. Raju, *Colloids Surf., A*, 2010, **367**, 31–40.
- 56 T. Wu, A. G. Xie, S. Z. Tan and X. Cai, *Colloids Surf., B*, 2011, **86**, 232–236.
- 57 Y. Ouyang, X. Cai, Q. S. Shi, L. L. Liu, D. L. Wan, S. Z. Tan and Y. S. Ouyang, *Colloids Surf., B*, 2013, 107, 107–114.

A table of contents entry



Pickering-based antibacterial hydrogels with tunable pore structures were fabricated by high internal phase emulsion templates.